

# Low-Energy Spectral Features in GRBs

Michael S. Briggs

*Department of Physics, University of Alabama in Huntsville, Huntsville, AL 35899*

---

I discuss low-energy lines in gamma-ray bursts. The process of deconvolving gamma-ray spectral data and the steps needed to demonstrate the existence of a line are explained. Previous observations and the current status of the analysis of the BATSE data are described.

---

Spectral lines are highly informative of the conditions of the region in which they are created. Unfortunately, the observational and theoretical understanding of lines in gamma-ray bursts is confused at best. Observations made with *Ginga* provided strong evidence for absorption lines, yet BATSE has not confirmed their existence. Confirmation of the existence of lines and a better characterization of their properties might provide the essential clue to the mystery of gamma-ray bursts.

In this paper I will not tell you whether lines exist, instead I will explain what analysis needs to be done to demonstrate the existence of a line in a gamma-ray spectrum to assist you in judging the evidence for yourself. I will briefly review selected observations and the status of the analysis of BATSE data. I will concentrate on observational issues regarding spectral features below 100 keV. The views expressed are my own.

## DETECTORS AND GAMMA-RAY INTERACTIONS

The detection of gamma-ray lines is much more difficult than the detection of optical lines, primarily because there is no one-to-one relationship between the energy of an incident gamma-ray photon and the energy measured by the detector, which is called the “energy loss”. Because of the difference between the energy of the incident photon and the energy loss, detected events are referred to as “counts”. Secondary problems are the poor signal-to-noise and signal-to-background ratios prevalent in gamma-ray astronomy.

The examples in this paper are from data collected with the Spectroscopy Detectors (SDs) of BATSE, but the concepts are true for all gamma-ray detectors—regardless of their energy resolution, the photon interaction physics is similar. The SDs are 12.7 cm diameter by 7.6 cm thick crystals of NaI(Tl) scintillator, each viewed by a photomultiplier tube (PMT) of the same diameter. When a gamma-ray interacts in the NaI crystal, a fraction of the resulting ionization energy is converted into scintillation light and measured by the PMT. In the energy range of interest, 10 keV to a few MeV, gamma-rays

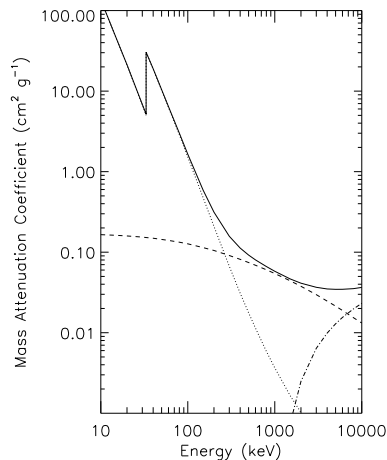


**FIG. 1.** The NaI gamma-ray mass attenuation coefficient  $\mu$ : solid line: total; dotted: photoelectric; dashed: Compton; dot-dash: pair production. The fractional transmission is  $\exp(-\mu x)$ , where  $x$  is the quantity of NaI traversed in  $\text{g cm}^{-2}$ . The data are from ref. (17).

interact with detector matter primarily by three processes (Fig. 1): photoelectric absorption, Compton scattering, and pair production (14,17,20).

In NaI, the photoelectric process dominates below  $\approx 200$  keV. In this process the gamma-ray is completely absorbed by an atomic electron. The interaction is most likely to occur with the inner-most electron that the gamma-ray has sufficient energy to ionize. Usually, an atomic cascade yields fluorescent X-rays, which will be photoelectrically absorbed unless they escape the crystal. Sometimes an Auger electron is ejected instead. The left curve of Fig. 2 illustrates a simple case, the detected energy losses expected from 20 keV photons. The fluorescent X-rays have a higher cross-section because of their lower energy (Fig. 1), so that they are unlikely to escape and thus the incident energy will be totally absorbed, leading to a simple observed spectrum. Broadening of the spectral resolution occurs, primarily due to Poisson fluctuations in the number of photoelectrons produced in the PMT (20).

A 50 keV photon is also most likely to interact via the photoelectric process, but the resulting count spectrum is more complicated (Fig. 2, bold curve). The inner-most shell of an iodine atom accessible to the 20 keV photon of the previous example is the L-shell. The K-shell becomes accessible to photons with energies above the K-shell binding energy of 33.17 keV, resulting in a cross-section increase (Fig. 1). A 50 keV photon will typically ionize a K-shell electron, resulting in a L, M or N to K shell transition and an X-ray with an energy between 28.3 and 33.0 keV (24). Sometimes this photon will interact by the photoelectric process and the total energy of the initial photon will be collected, resulting in the full-energy absorption peak at the right in the bold curve of Fig. 2. However, the fluorescence X-ray is below the K-edge and has a lower cross-section (Fig. 1) and thus a high probability of escaping the crystal, resulting in incomplete absorption of the energy of the incident gamma-ray (the left peak of the bold curve of Fig. 2).

Comparing incident photon energies just above and below the 33.17 keV K-

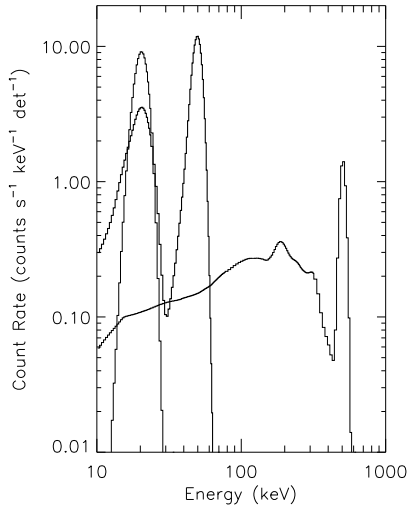


**FIG. 2.** Simulated instrumental energy loss spectra, commonly known as count loss spectra, for monoenergetic photons incident on a Spectroscopy Detector, the detector’s surroundings on CGRO and the Earth’s atmosphere. The simulation matches the conditions with which SD 5 observed GRB 920311 (BATSE trigger 1473), except for clarity the simulated data extend to energies slightly below where the current calibration is reliable. (Data from SD 5 and GRB 920311 are shown in Fig. 3.) In each case the input flux is  $1 \text{ photon s}^{-1} \text{ cm}^{-2}$ . Left curve: photon energy 20 keV; middle, bold curve: 50 keV; right curve: 500 keV.

edge of iodine, the higher energy photon has a higher interaction probability, but more importantly, a lower probability of complete energy absorption. For a hard incident spectrum, such as a GRB spectrum, this K-edge effect results in a deficit from 33 to  $\approx 50$  keV in the count spectrum, which appears as a peak at  $\approx 30$  keV and is predicted by the detector response model (see Fig. 3). This feature has been used as a verification of the calibration of the SDs (32) and should not be mistaken for an astrophysical line.

At 500 keV, photoelectric absorption occurs only  $\approx 20\%$  of time, making a contribution to the full-energy absorption peak (see Fig. 2, right curve). The most likely interaction is Compton scattering, which transfers only a portion of the incident photon’s energy to an electron. Complete energy absorption will occur only if additional interactions occur, either photoelectric or Compton. In Compton scattering the maximum energy transfer to the electron, 331 keV, occurs when the incident photon is scattered  $180^\circ$ . A range of scattering angles approaching  $180^\circ$  creates the peak in the curve at 310 keV and the lack of larger energy transfers in single scattering events causes the valley above 331 keV (see Fig. 2). Correspondingly, the minimum energy of a scattered photon is 169 keV, so a range of angles approaching  $180^\circ$  for incident photons that *scatter into* the detector from the spacecraft or the Earth’s atmosphere creates the peak at 190 keV.

At yet higher energies pair production becomes important.

## SPECTRAL DECONVOLUTION AND LINE DETECTION

As described in the previous section, an observed 20 keV count could be due to a 20, a 50, or even a 500 keV photon! When a single count is observed, it is impossible to deduce the energy of the incident photon. If many counts

are observed, the incident spectrum can be deduced within statistical limits in the process known as deconvolution.

We approximate the continuous (as a function of energy) detection process with the following discrete equation:

$$\vec{c} = \mathbf{D}\vec{p}. \quad (1)$$

Here  $\vec{c}$  is the vector with the counts versus energy bins. Normally these data are only available in binned form in order to reduce telemetry requirements—as long as the energy bin widths are small compared to the detector’s energy resolution essentially no information is lost. Similarly,  $\vec{p}$  is the vector representing the incident photon spectrum. The detector is represented by  $\mathbf{D}$ , the detector response matrix, which is obtained via Monte Carlo simulations of gamma-ray interactions in a computer model of the detector (e.g., (35)).

The obvious solution is

$$\vec{p} = \mathbf{D}^{-1}\vec{c}. \quad (2)$$

This simple approach does not work if one wishes to deduce information at a resolution at or better than the intrinsic resolution of the detector, which is the goal of analyzing data for the presence of lines. The problem is that if the energy widths of the rows and columns of  $\mathbf{D}$  are comparable to the detector resolution, then neighboring columns will be very similar and  $\mathbf{D}$  will be nearly singular. Inverting  $\mathbf{D}$  will be numerically unstable and the solution  $\vec{p}$  will be unreliable, especially in the presence of statistical fluctuations in the observed count spectrum  $\vec{c}_{\text{obs}}$ .

Instead, the standard approach in astrophysics has become that of forward-folding (38,11,25). A parameterized spectral model is *assumed* and used to calculate  $\vec{p}_{\text{model}}$ , from which eq. 1 yields a model count spectrum  $\vec{c}_{\text{model}}$ . The model count spectrum  $\vec{c}_{\text{model}}$  is compared to the observed count spectrum  $\vec{c}_{\text{obs}}$  using some statistical measure such as  $\chi^2$  or likelihood and the parameters of the photon model are optimized so as to minimize the discrepancy between  $\vec{c}_{\text{model}}$  and  $\vec{c}_{\text{obs}}$  according to the chosen statistical measure.

It is very important to realize that a solution obtained by forward-folding is not unique but is rather photon model dependent (11,25). Even if a model fit results in a good  $\chi^2$  value, another, possibly unknown, model might result in an equal or better  $\chi^2$  value. This is shown in Fig. 3, where solutions ‘a’ and ‘b’, based upon different photon models, have essentially identical  $\chi^2$  values. What a forward-folding solution provides is the parameter values of the *assumed* photon model (25).

In gamma-ray astrophysics, deconvolved photon points are frequently obtained by scaling the model photon spectrum by the ratio of the observed over modeled counts (25)—Fig. 3 (right) is an example. This practice is potentially misleading because the deconvolved points are model dependent yet there is an almost irresistible temptation to regard them as incident spectrum “data” points. In the examples in Fig. 3, based upon alternative continuum

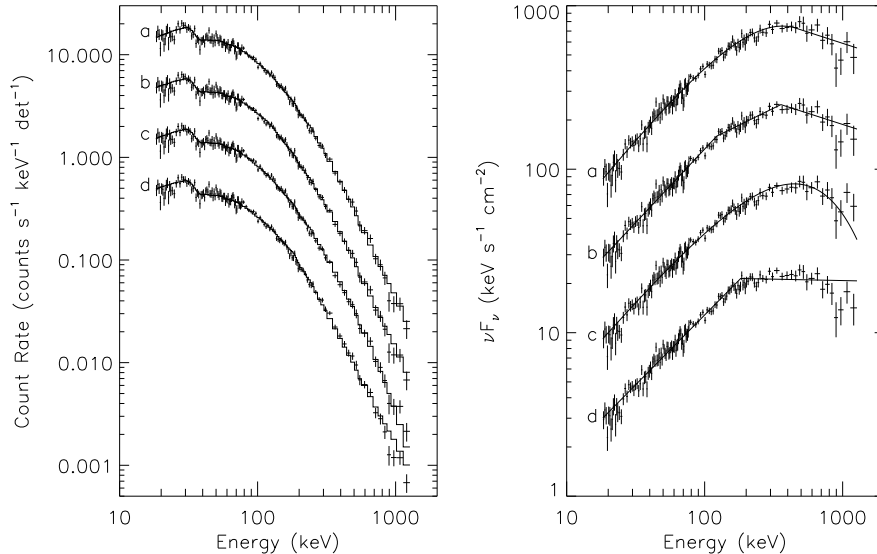


**FIG. 3.** To illustrate the photon model dependent nature of the forward-folding deconvolution method, identical data is analyzed using four different photon models. Model ‘a’ assumes Band’s spectral form (2), obtaining  $\chi^2=223$  for 200 degrees-of-freedom (dof). Model ‘b’ is a power-law with two breaks;  $\chi^2=227$  for 198 dof. Model ‘c’ is a power law times an exponential cutoff;  $\chi^2=244$  for 201 dof. Model ‘d’ is a power-law with one break;  $\chi^2=267$  for 200 dof. The data are for the interval 1.088 to 26.624 s of GRB 920311 as observed by SD 5; above 200 keV, the data have been rebinned into wider channels for display purposes. Each group after ‘a’ is shifted downwards by  $\times\sqrt{10}$ . Left: count data (points) and models (histograms). Right: Deconvolved points and models. The  $\nu F_\nu$  spectrum is  $E^2 \times$  the photon flux spectrum. The photon models obviously differ—there are also differences in the values of the deconvolved points, e.g., the values of right-most point are  $483 \pm 101$ ,  $483 \pm 101$ ,  $593 \pm 113$  and  $449 \pm 98$   $\text{keV s}^{-1} \text{cm}^{-2}$  for models ‘a’, ‘b’, ‘c’ and ‘d’, respectively.

models, the differences in the deconvolved points are subtle and the practice not too pernicious. When a line with width comparable to or smaller than the detector’s intrinsic resolution is considered, the deconvolved spectra can exaggerate the significance of a line—see Fig. 4. Papers analyzing spectra in the X-ray band generally show a graph of the count data and model and a graph of the residuals (e.g., (22)). Only rarely is a graph of a deconvolved spectrum presented. The gamma-ray community is advised to emulate this practice.

Because of the limitations of gamma-ray spectral data, the following steps are necessary to demonstrate that a line feature exists:

- *Deconvolve spectra using the forward-folding technique.* This is the standard approach in X-ray and gamma-ray spectroscopy.

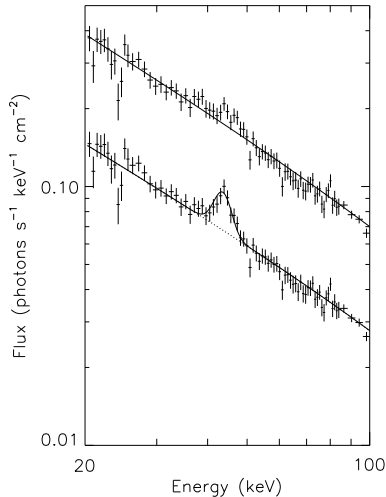


**FIG. 4.** To illustrate the dependence of the deconvolved photon points on the model for a model containing a line, two deconvolutions of the same data are shown. For the top curve, a continuum model is assumed, while for the bottom curve (shifted downward by  $\times 2.5$ ), an additive Gaussian line is also included in the model. The data are that of the line candidate in GRB 940703—for count data and models see ref. (9).

- *Show the data and the model in counts rather than deconvolved photons.* The fit is performed by comparing observed and model counts and the data and model should be displayed in this space.
- *Show that the line is significant versus all reasonable continuum models.* Suppose that  $\Delta\chi^2$  indicates that a line is a statistically significant improvement to continuum model A—one might be tempted to say that the line is “proven”. However, if the line insignificantly improves continuum model B *and* model B has comparable  $\chi^2$  to that of A+line, then we cannot say the line must exist because continuum model B may be the correct explanation. Since we do not know the correct continuum model of GRBs, we must try all reasonable ones (11,12); since all models cannot be tried, judgement is needed. In practice, this means that a sufficiently flexible continuum model should be used (12). With current data, an appropriate choice for all bursts is Band’s function (2,5), which is usually the best-fitting model for bright bursts (e.g., Fig. 3). A power law with multiple breaks is also sufficiently flexible, but has the disadvantage of not being smooth. An evolving or two-component continuum spectrum might mimic a line when a single continuum model is used for the analysis (16,36).
- *Provide a quantitative evaluation of the statistical significance of the feature.* Without such an evaluation one does not know the strength of the evidence that a line is real rather than a fluctuation. It has been traditional to use the F-test (e.g., (12,8,33)), but the BATSE team has recently realized that  $\Delta\chi^2$  is more appropriate for this case, where one knows the uncertainties from Poisson statistics (23,10,7). In evaluating the significance of a feature, the number of trials should be considered.
- *Consider possible systematic errors.* Does the line centroid match that

of a background line? If so, is the background subtraction adequate? Is the detector model and calibration adequate?

- *If possible, evaluate the feature for confirmation/consistency.* If more than one instrument, or more than one detector of an instrument, observed the burst with appropriate energy coverage and resolution, then the two observations should be compared. Ideally, both detectors would show the feature to be statistically significant, thereby confirming the detection. Depending on the sensitivity of the detectors and the strength of the burst, this may not be possible. In any case, consistency between the data of the two detectors is required.

## LINE OBSERVATIONS

Table 1 summarizes the analyses methods used in previous observations of gamma-ray burst spectral features below 100 keV and Table 2 presents the results of those analyses. Many of the previous analyses were done before the gamma-ray community realized the importance of all of the steps listed in the previous section and before computer improvements made the forward-folding approach practical. Probably due to improvements in the sensitivity of detectors, there has been historical progression towards continuum models with more parameters (5). Many of the earlier line analyses were done using continuum models that are now known to be too simple, raising the possibility that the line detections are an artifact of the chosen continuum model. Unfortunately, these problems mean that some of the previous analyses must now be judged as inconclusive with regard to the existence of gamma-ray burst lines. Considering the importance of this question, reanalyses are merited.

The Konus observations pioneered GRB line studies. The analysis technique was cleverly designed to minimize the computations required: the count spectra were deconvolved using a standard model and the resulting photon spectra were iteratively improved (28). The continuum model used was optically thin thermal bremsstrahlung,  $\propto E^{-1} \exp -E/E_0$ . The explanation of the deconvolution procedure shows one count spectrum as an example (28). It has been frequently suggested that the Konus lines might be harmonics of fundamentals that are below the typical detector threshold of 30 keV.

**TABLE 1.** Low-Energy Spectral Features: Analysis Methods

Instrument	References	Forward-Folding used?	Count Data & Model shown?	Flexible Continuum Model used?	Statistical Significance evaluated?
Konus	(26-28)	No	No	No	No
HEAO A-4	(18,19)	No	No	No	Yes
<i>Ginga</i>	(12,15,31,39,40)	Yes	Yes	Yes	Yes
Lilas	(8)	Yes	No	Yes	Yes

**TABLE 2.** Low-Energy Spectral Features: Results

Instrument	GRB	References	$\Delta\chi^2$	Centroids (keV)	equiv. width (keV)
Konus	many <sup>a</sup>	(26–28)		30–70	5–15
HEAO A-4	780325 <sup>b</sup>	(19)	14.0	76±5	24
	780325 <sup>c</sup>	(19)	16.6	49±3	13
	780608	(19)		66±7	14
<i>Ginga</i>	880205	(31,12)	48.5	19.7±0.7, 38.0±1.6	3.7, 9.1
	870303 <sup>d</sup>	(15)	30.6	21.1±1.1	10.5
	870303 <sup>e</sup>	(31,15)	26.2	21.4±0.7, 2×21.4	4.8, 8.4
	890929	(40)	25.6	26.3±1.5, 46.6±1.7	4, 8
Lilas	890306	(8)	89.0	11.2±0.5, 34.6±1.4	

<sup>a</sup>Unique amongst the results listed in this table, one GRB had an emission feature.

<sup>b</sup>First peak of the burst.

<sup>c</sup>Second peak of the burst.

<sup>d</sup>Interval ‘S1’.

<sup>e</sup>Interval ‘S2’.

The most significant line in the HEAO A-4 data is in the 2<sup>nd</sup> peak of GRB 780325 (19). The line significance was evaluated using a simple continuum model, an exponential, fit to only the data below 200 keV (19). Using a better model and all of the data might raise or lower the significance. The deconvolution was done using photons-to-counts efficiencies derived for an  $E^{-2}$  spectrum, a procedure equivalent to approximating  $\mathbf{D}$  with a diagonal matrix. This procedure was justified by the suppression of the Compton scattering response by the active shielding of the instrument and has the advantage of conservatively assuming that lines do not exist. The feature is stated to be visible in two detectors, but only summed data are shown (19).

The analysis of the *Ginga* data is excellent. (However, some papers present only deconvolved spectra.) The chance probability of obtaining a reduction in  $\chi^2$  of 48.5 by adding two lines, assuming that the lines do not exist, is  $10^{-8}$ ! The harmonic relation between the line centroids is powerful evidence for the cyclotron resonant scattering interpretation. A possible concern is that the lines were in the same channels in all 3 bursts (13)—while the centroid energies are different in GRB 890929, for this event the gains of the detectors were lower than normal (40).

The recent results of Lilas on GRB 890306 are even more statistically significant—lines at 11 and 35 keV are reported in a 68 s interval with an F-test probability of  $2 \times 10^{-13}$  that this is a chance result (8). The  $\chi^2$  value for the model containing the lines is somewhat high: 43.2 for 26 degrees-of-freedom. This  $\chi^2$  value, along with the location of one line near the detector threshold and the other near the iodine K-edge, are areas for concern. It would be desirable to see the count model for these data and also for a comparable spectrum not containing lines. The spectral evolution during the 68 s



interval, which is essentially the entire burst, should also be investigated.

### BATSE AND LINES

The Spectroscopy Detectors were added to BATSE because of the Konus line observations. The pre-launch expectations of the BATSE team were that lines would be readily found. Simulations (3) and performance tests (32) verify the ability of BATSE to detect *Ginga*-like lines, with generally poorer sensitivity than *Ginga* for 20 keV lines and better for 40 keV lines. However, no lines have been detected with BATSE (33,4). While disappointing, this lack of line detections by BATSE is not yet in strong contradiction with the observations of *Ginga* (33,4,6).

BATSE has a number of advantages for line studies:

- State of the art scintillation detectors: excellent energy resolution and advanced electronics incorporating active PMT bleeder strings and baseline restoration to handle large pulses and high count rates,
- Excellent temporal resolution so that lines can be found on whatever time scale they may exist,
- GRB locations from the LADs to aid analysis of the SD data,
- Good sensitivity,
- Extensive performance verification, on the ground and in-orbit (32),
- Multiple detectors and detector types, which enable consistency/confirmation studies,

The BATSE team is therefore confident of the instrument's ability to detect lines. Because of the lack of detections by the initial approach, visually examining burst spectra for lines (33), the team has implemented the most thorough line search ever conducted. This comprehensive computer search examines essentially all time scales and energy centroids below 100 keV. The new approach has already identified 8 candidate features with  $\Delta\chi^2 > 20$  (9). Currently analysis is in progress to determine the consistency of the multi-detector data and hopefully to confirm some of the features with multiple detectors. Until that work is completed the BATSE team considers these features to be candidates rather than detections.

### THE FUTURE

There is much more work to be done. On the interpretational side, bursts from galactic halo or cosmological distances have intrinsic luminosities  $10^4$  or more greater than deduced in the days of the galactic disk paradigm. Consequently, the physics of line creation will be different than previously envisioned. This has been examined in the context of sources in the galactic halo (e.g., (21)), but little work has been done in the context of cosmological models. Several of the past line observations merit reanalysis using techniques

developed since they were published. The analysis of the BATSE data continues in order to determine the reality of the candidates identified by the comprehensive search. With eight candidates already identified, and typically several high-gain SDs viewing a burst, the BATSE team will be able to determine the consistency of the data and confirm many of the candidate features or to demonstrate that there is some problem. Data are also currently being collected and analyzed with the scintillation detectors of the Konus-W instrument (1,29) and the high energy-resolution detectors of TGRS (34). The near future will bring the launch of HETE (37) and PGS on Mars-96 (30).

## REFERENCES

1. R. L. Aptekar, D. D. Frederiks, et al., in AIP Conf. Proc. **366**, 158, (1996).
2. D. Band, J. Matteson, L. Ford, et al., ApJ **413**, 281 (1993).
3. D. L. Band, L. A. Ford, J. L. Matteson, et al., ApJ **447**, 289 (1995).
4. D. L. Band, S. Ryder, L. A. Ford, et al., ApJ **458**, 746 (1996).
5. D. L. Band, these proceedings (1996).
6. D. L. Band, L. Ford, et al., these proceedings (1996).
7. D. L. Band, et al., "BATSE Gamma-Ray Burst Line Search: V. Probability of Detecting a Line in a Burst", ApJ, submitted (1996).
8. C. Barat, A&A Suppl. Ser. **97**, 43 (1993).
9. M. S. Briggs, R. D. Preece, G. N. Pendleton, et al., these proceedings (1996).
10. W. T. Eadie, D. Drijard, F. E. James, M. Roos & B. Sadoulet, Statistical Methods in Experimental Physics, New York: North-Holland (1971).
11. E. E. Fenimore, R. Klebesadel & J. Laros, Adv. Space. Res. **3**, #4, 207 (1983).
12. E. E. Fenimore, J. P. Conner, R. I. Epstein, et al., ApJ **335**, L71 (1988).
13. E. E. Fenimore, private communication.
14. E. Fermi, Nuclear Physics, rev. ed., Univ. of Chicago Press (1950).
15. C. Graziani, E. E. Fenimore, T. Murakami, et al., in Gamma-Ray Bursts, ed. C. Ho, R. I. Epstein & E. E. Fenimore, Cambridge Univ. Press, 407 (1992).
16. A. K. Harding, et al., in AIP Conf. Proc. **141**, 98 (1986).
17. J. H. Hubbell, Photon Cross Sections, Attenuation Coefficients, and Energy Absorption Coefficients from 10 keV to 100 GeV, Nat. Bureau of Stand. (1969).
18. G. J. Hueter, in AIP Conf. Proc. **115**, 373 (1984).
19. G. J. Hueter, Ph.D. Thesis, University of California, San Diego (1987).
20. G. F. Knoll, Radiation Detection and Measurement, 2nd ed., Wiley (1989).
21. M. Isenberg, D. Q. Lamb & J. C. L. Wang, these proceedings (1996).
22. K. Koyama, R. Petre, E. V. Gotthelf, et al., Nature **378**, 255 (1995).
23. D. Q. Lamb, private communication (1995).
24. C. M. Lederer, et al., Table of Isotopes, 7th ed., New York: Wiley (1978).
25. T. J. Loredo & R. I. Epstein, ApJ **336**, 896 (1989).
26. E. P. Mazets, S. V. Golenetskii, et al., Nature **290**, 378 (1981).
27. E. P. Mazets, S. V. Golenetskii, V. N. Ilyinskii, et al., Ap&SS **82**, 261 (1982).
28. E. P. Mazets, S. V. Golenetskii, et al., in AIP Conf. Proc. **101**, 36 (1983).
29. E. P. Mazets, R. L. Aptekar, D. D. Frederiks, et al., these proceedings (1996).
30. I. G. Mitrofanov, et al., Adv. Space Res. **17**, #12, 51 (1996).
31. T. Murakami, M. Fujii, K. Hayashida, et al., Nature **335**, 234 (1988).

- 32. W. S. Paciesas, M. S. Briggs, R. B. Wilson, et al., these proceedings (1996).
- 33. D. M. Palmer, B. J. Teegarden, B. E. Schaefer, et al. *ApJ* **433**, L77 (1994).
- 34. D. M. Palmer, H. Seifert, B. J. Teegarden, et al., these proceedings (1996).
- 35. G. N. Pendleton, et al., *Nucl. Instr. & Meth. in Phys. Res.* **A 364**, 567 (1995).
- 36. G. N. Pendleton, M. S. Briggs, R. D. Preece, et al., these proceedings (1996).
- 37. G. R. Ricker, J. P. Doty, S. A. Rappaport, et al., in *Gamma-Ray Bursts*, ed. C. Ho, R. I. Epstein & E. E. Fenimore, Cambridge Univ. Press, 288 (1992).
- 38. J. I. Trombka, *Nature* **226**, 827 (1970).
- 39. J. C. L. Wang, D. Q. Lamb, et al., *Phys. Rev. Lett* **63**, 1550 (1989).
- 40. A. Yoshida, et al., in *Gamma-Ray Bursts*, ed. C. Ho, R. I. Epstein & E. E. Fenimore, Cambridge Univ. Press, 399 (1992).